FOREX Publication
Open Access | Rapid and quality publishing

International Journal of
Electrical and Electronics Research (IJEER)
Research Article | Volume 13, Issue 3 | Pages 487-492 | e-ISSN: 2347-470X

Investigating a Broadband Microstrip Patch Antenna that Demonstrates Enhanced Bandwidth for 5G-Based Applications

Anagh Sankar Das[1*], Aditya Goel[2] and Sangeeta Nakhate[3]

[1]*PhD Scholar, Department of ECE, Maulana Azad National Institute of Technology, Bhopal, India; Email: anaghsankardas@gmail.com*
[2]*Professor, Department of ECE, Maulana Azad National Institute of Technology, Bhopal, India; Email: adityagoel2@rediffmail.com*
[3]*Associate Professor, Department of ECE, Maulana Azad National Institute of Technology, Bhopal, India; Email: sanmanit@gmail.com*

***Correspondence:** anaghsankardas@gmail.com;

ABSTRACT- This paper presents a dual-fed approach to the design of a wide bandwidth microstrip patch antenna (MPA) of patch dimensions (l × w = 42 mm × 37 mm) and substrate dimensions (l × w × h = 100 mm × 100 mm × 3.14 mm); featuring two symmetrically inverted U-slots of dimensions (l × w × h = 25.62 mm × 15.5 mm × 2 mm) and two coaxial probes (7 mm each) adjacent to each slot. The substrate material utilized is Rogers-RT/duroid-5880, exhibits a dielectric constant of 2.2, makes it extremely efficient in reducing lossy nature of generated output parameters. The antenna demonstrates broad -10 dB impedance bandwidth ≈ 44% from 2.55 GHz - 3.85 GHz centered at a frequency of 3 GHz within the S band (2-4 GHz) region. A radiation intensity of 12 dB is observed alongside impeccable efficiency of 99.98%. Comparative analysis against various configurations underscores a significant enhancement in bandwidth at a specific resonant frequency, facilitated by numerical assessment of patch dimensions. Notably, the resonant frequency aligns exactly with the antenna's center frequency of 3 GHz, displaying a voltage standing wave ratio (VSWR) value nearing unity (≈1), indicative of favorable impedance matching conducive to enhanced wideband performance. Fairly symmetrical radiation patterns and a gain approaching 6 dB at the designated frequency further characterize the antenna's performance. This design holds promise for diverse applications including wireless local area network (WLAN), Worldwide Interoperability for Microwave Access (WiMAX) and 5G-based applications, like internet-of-things (IoT) and satellite communications as affirmed by the congruence between simulation and measurement results, which were obtained using a vector network analyzer (VNA) after procuring the desired hardware model using chemical etching procedure. Simulations are executed using High Frequency Structure Simulator (HFSS) simulation tool that utilizes finite element method (FEM) technique to undergo its mesh operations.

Keywords: Microstrip patch antenna, impedance bandwidth, gain, VNA, HFSS, FEM.

ARTICLE INFORMATION

Author(s): Anagh Sankar Das, Aditya Goel and Sangeeta Nakhate;
Received: 28/11/2024; **Accepted**: 05/07/25; **Published**: 30/08/25;
E- ISSN: 2347-470X;
Paper Id: IJEER240438;
Citation: 10.37391/ijeer.130313
Webpage-link:
https://ijeer.forexjournal.co.in/archive/volume-13/ijeer-130313.html

crossref member
CROSSREF.ORG THE CITATION LINKING BACKBONE

Publisher's Note: FOREX Publication stays neutral with regard to jurisdictional claims in Published maps and institutional affiliations.

1. INTRODUCTION

Since the early 1970s, when microstrip patch antennas were first introduced, numerous studies have been conducted to increase their bandwidth. Well-known techniques such as thickening the substrate or using a substrate with a lower contrast dielectric can be used to increase the bandwidth. Placing parasitic patches in various layers [1, 2] will also increase bandwidth; these approaches produce stacked or coplanar layouts, respectively. While coplanar arrangement increases the antenna's dimensions, stacked arrangement does not meet some of the key benefits of patch antennas, such as low profile and ease of fabrication. Much work has been done to increase the impedance bandwidth of single-layer patch antennas. Furthermore, the investigators have concentrated on ascertaining the characteristics of these U-slot patch antennas [3–8]. Other models, such as half U-slot patch antennas [9], C-shaped [10], E-shaped [11], and ψ-shaped [12], were also proposed in addition to the U-slot model. In addition to these techniques, researchers have concentrated on relocating feeding points to increase bandwidth [13–19]. Due to their low profile and lower cost when compared to other antennas. Microstrip patch antennas are typically lightweight and in high demand due to their ease of fabrication. Slot-loaded patch antennas have a wide range of applications in wireless communications. This is mostly since they are, in comparison to other antennas, more affordable, and because of their low-profile design. In general, microstrip patch antennas are lightweight and in high demand because they are simple to fabricate and because their production process is significantly less complicated. There is another name for these antennas, which are printed antennas. Most of it is made up of a rectangular metal sheet that has been flattened, which is essentially the "patch" as it is often referred as. A substrate, which is also referred to as a dielectric substance, is used to attach this patch [20]. At the bottom of the substrate is another metal layer that acts as the ground plane.

Open Access | Rapid and quality publishing

International Journal of Electrical and Electronics Research (IJEER)
Research Article | Volume 13, Issue 3 | Pages 487-492 | e-ISSN: 2347-470X

The process of radiation occurs because of the phenomenon known as fringing, which allows the antenna to function electrically in a manner that is somewhat bigger than its actual physical size. Utilising a patch that is just half the wavelength in length is the antenna that offers the greatest degree of convenience. Normally, microstrip patch antennas are available in various shapes and sizes. They can either be elliptical, or they can be rectangular in size, or sometimes even circular. Apart from all these shapes and sizes, various other shape variations are also obtainable. Moreover, an antenna can also be made by creating any random continuous shape, provided radiation takes place properly from the structure. In general, ground planes which are electrically largeish, generate very sturdy patterns and they also enhance the antenna dimensions. Generally, it is not rare that the size of the ground plane is just a little bigger than the patch itself. If the ground plane size is anywhere close to the radiator size, then it can cause an event where coupling takes place, thereby generating current along the peripheries of the plane that can radiate too.

A pattern in an antenna is formed as a pair of sets of radiating metal elements get combined to make such an occurrence. The radiation can be thought of as being generated by some slots that can radiate from the top as well as the bottom surface, or sometimes even together at the same time due to current flow on the patch and ground plane. In recent times, there has been a significant amount of interest in the applications that fall under the S-band (2-4 GHz) [21] spectrum. These applications include satellites for communication, radars for accurate weather prediction, radars used in ship surfaces, wireless local area networks (WLAN), and for its applications in multimedia, such as mobile TV and radio for satellites, among other things. Studies are being carried out in a methodical manner to construct low profile patch antenna arrays [22]. These arrays are designed to provide greater S-band broad bandwidth, frequency duality or reconfigurability, and huge gain to make them very relevant to the S-band area [23].

2. DESIGN MECHANISM AND MATHEMATICAL MODELLING

A rectangular MPA is easily accomplished by cutting out a slot at a desirable location in a patch, that is operable on a comparatively lesser dielectric constant and a thicker substrate. In order to enhance the impedance bandwidth, the required patch antenna is designed by placing symmetrically a couple of opposite-faced U-slots, located at equal distances from the center as shown in *figure 1* and *2*. The one additional *slot*, accounts for the *symmetricity* of the antenna radiation pattern and is also responsible for creating a greater bandwidth in comparison to a usual patch antenna which makes it much more applicable for various wireless applications for instance WLAN, Bluetooth, WiMAX and for various other applications in the S-band region ranging from air traffic control, satellites for space communication and weather radar. The design of this model leading to higher broadside radiation for magnified data coverage was mostly determined by enhancements in substrate height and patch width.

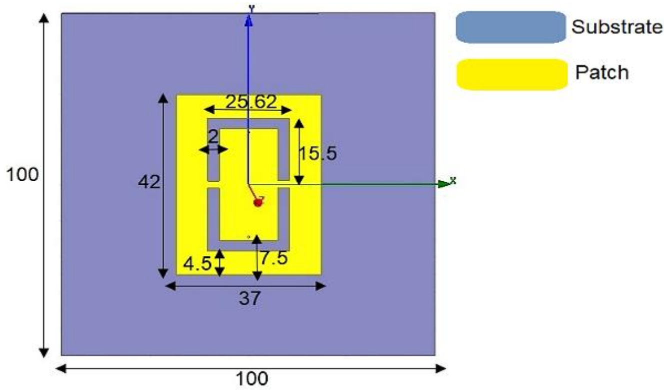

Figure 1. Aerial view of the patch antenna

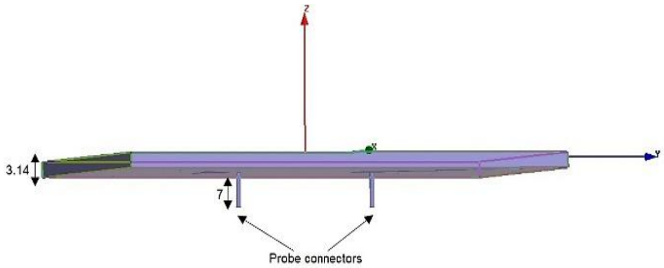

Figure 2. Side view of the patch antenna

Table 1. Patch Measurement Specifications

Parameter	Measurement (in mm)
Patch length	42
Patch width	37
Feeding Point distance on Patch	7.5
Slot length	25.62
Slot width	15.5

The measurements that were considered to simulate the patch antenna design are listed in *table 1*. Following several iterations, the previously indicated design parameters were determined to be the most appropriate for producing optimised trade-off accounting for the creation of wide bandwidth overall. Maintaining a proportionate spacing between probe-feed structures is necessary to prevent errors in radiation patterns and to maintain the quality of the bandwidth produced. These measurements can be seen later in the simulated design of this model.

2.1. Length of Patch

$$L \approx \frac{1}{2f_r\sqrt{\varepsilon_0 \varepsilon_r u_0}} \quad (1)$$

Here, the length of patch is assigned as L and μ_0 symbolises permeability of free space, whereas ε_0 denotes permittivity free space. f_r indicates the resonant frequency of the antenna, while ε_r denotes permittivity of the Rogers-RT/duroid-5880 substrate.

(ε_0=8.85 × 10^{-12} Fm^{-1} and μ_0 =1.257 x 10^{-6} Hm^{-1})

2.2. Effective Patch Length

$$L_{eff} = L + 2\Delta L \quad (2)$$

The effective length of the patch antenna is symbolized by L_{eff} and L denotes actual patch length. This is important because the effect of fringing causes the patch to behave a little larger than its real dimensions, electrically. ΔL is the extension in patch length.

2.3. Extension in Length of Patch

As mentioned before, the fringing effect causes increase in patch length.

$$\Delta L = h\,(0.412)\frac{(\varepsilon_{reff}+0.3)}{(\varepsilon_{reff}-0.258)}\left(\frac{\frac{w}{h}+0.264}{\frac{w}{h}+0.8}\right) \quad (3)$$

ΔL denotes extension in length of patch, as mentioned earlier that happens because of fringing. The patch width and substrate height are denoted by w and h respectively, in the above equation. ε_{reff} denotes effective permittivity.

2.4. Resonant Frequency

$$f_r \approx \frac{c}{2L\sqrt{\varepsilon_r}} \quad (4)$$

In the above equation, f_r indicates resonant frequency, ε_r signifies permittivity of Rogers RT/duroid 5880 substrate material ($\varepsilon_r = 2.2$) and L denotes patch length, while c indicates speed of light ($c = 3\times10^8$ m/s).

2.5. Computation of Effective Permittivity

$$\varepsilon_{reff} = \frac{\varepsilon_r+1}{2} + \frac{\varepsilon_r-1}{2}\left[1+12\left(\frac{h}{w}\right)\right]^{-1/2} \quad (5)$$

The effective permittivity after fringing takes place in a medium, ultimately turns out to be ε_{reff} as shown in the above equation.

2.6. Bandwidth Percentage computation for designed model

$$Bnd = (f_{High} - f_{Low})/f_r \quad (6)$$

Effective bandwidth % is evaluated using the above eq. where Bnd signifies % bandwidth, f_{High} and f_{Low} denote start and end values of freq at the concerned bandwidth and f_r being resonant freq.

2.7. Antenna efficiency

When accounting for losses at the input terminals of the antenna, which include conduction and dielectric losses as well as mismatch reflections between the transmission line and the antenna, the formula for antenna efficiency (η) may be expressed as follows:

$$\eta = P_{accept} / P_{input} = 1-|\Gamma|^2 \quad (7)$$

Γ represents voltage reflection coefficient at the antenna input terminals and can be determined by

$$\Gamma = \frac{Z_{in}-Z_0}{Z_{in}+Z_0} \quad (8)$$

where Z_{in} indicates input impedance of antenna and Z_o is the characteristic impedance of transmission line.

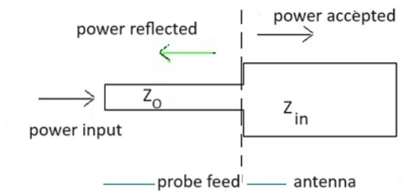

Figure 3. Determination of antenna efficiency

2.8. Voltage Standing Wave Ratio

VSWR is an abbreviation that stands for Voltage Standing Wave Ratio. Impedance matching is a technique used in radio frequency engineering to assess how well a load, such as an antenna or transmission line, matches the input impedance of the transmission line that supplies it. VSWR, or Voltage Standing Wave Ratio, is a measurement that quantifies the ratio between the highest and lowest voltages found along a transmission line. This ratio is caused by the existence of standing waves that develop owing to differences in impedance. Mathematically, it can be represented as

$$VSWR=(1+|\Gamma|)/(1-|\Gamma|) \quad (9)$$

3. RESULTS AND DISCUSSION

The patch antenna has a size of (l × w = 42 mm × 37 mm) and it is put on top of a substrate which consists of material Rogers RT/duroid 5880. It has a thickness of 3.14 mm. A layer of perfect electric conductor (PEC) is deposited underneath the substrate. This layer functions as a foundation. Dimensions of the substrate are (l × w × h = 100 mm × 100 mm × 3.14 mm). Using two identically magnitude 50-ohm probes, the substrate is fed coaxially. The two probes should be positioned at equal distances from the patch's center to generate the antenna's symmetrical radiation pattern.

3.1. Effect on Antenna Bandwidth via modification to design input parameters

It is well recognised that altering the length of a patch leads to a change in the resonance frequency of the output. We have shown many instances to substantiate this assertion. Furthermore, we have made modifications to the patch width or height in specific circumstances, while maintaining the integrity of the substrate material. We have conducted a comprehensive analysis, comparing each of them to the original parameters of our design. This revealed that the impedance matching for the antenna is almost lossless, resulting in a higher bandwidth. and corresponds to a value of 43.33% for the proposed design. The antenna's impedance bandwidth range is -10dB and spans from 2.55 to 3.85 GHz as shown in *figure 4*.

Research Article | Volume 13, Issue 3 | Pages 487-492 | e-ISSN: 2347-470X

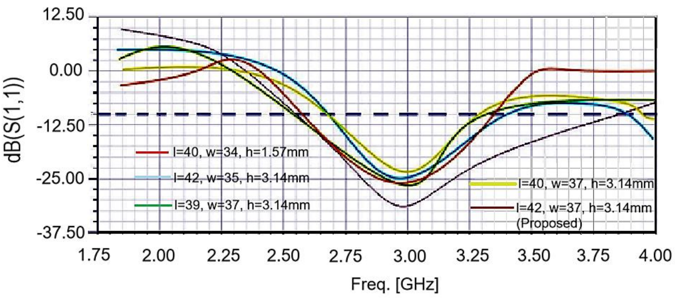

Figure 4. Bandwidth analysis for Antenna through return loss evaluation by changing specified antenna dimensions

3.2. Effect on Input Impedance using Smith Chart

Impedance value in the Smith chart is impacted by changes in antenna parameters, just as it was in the preceding instances. This is highly significant for the antenna's impedance matching. It is a very useful tool that can be used in any area of radio frequency engineering. The most widely used version of this chart is the impedance Smith chart. As shown in *figure 5*, its importance in determining the input impedance of a designed antenna does not diminish even with the introduction of different simulation softwares.

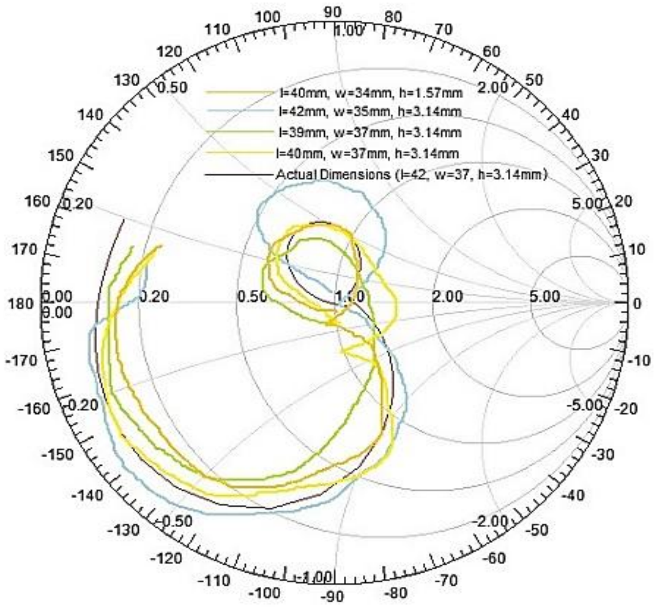

Figure 5. Smith chart impedance variation by changing Antenna dimensions

3.3. Effect on Distribution of Electric & Magnetic Field for Patch

The distribution of the electric field is impacted by parameter changes, that is shown in *figure 6*. The area next to the slots has no magnitude. Thus, we can conclude that the differences in these fields only occur within the vicinity of the slots, not outside of them. Similarly, a current vector distribution plot is shown for the same, where the patch region's traveling current direction is indicated by the series of arrows.

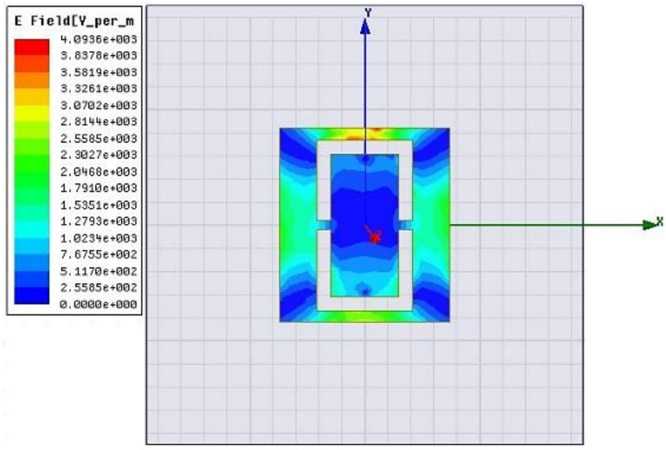

Figure 6. Electric field distribution for proposed design

3.4. Effect on the Antenna Pattern of Radiation

The suggested design's E and H-plane radiation patterns are shown in *figure 7(a)* and *7(b)*, which were previously covered in earlier sections, are crucial for determining the maximum range over which radiation occurs. It is evident that the patterns progressively approach the output's original dimensions. An antenna's radiation pattern is a crucial component in identifying its type of radiation, and the antenna's ability to radiate will depend on how much the pattern varies. As can be seen from the readings, radiation intensity has a maximum value of 12 dB and is perfectly symmetric for E-field patterns and closely symmetric for H-field patterns.

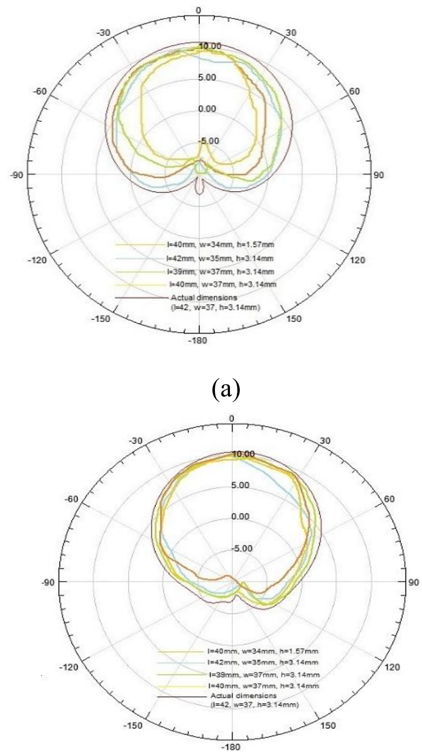

(a)

(b)

Figure 7. Antenna Radiation Patterns of proposed design for (a) E-field, (b) H-field

International Journal of
Electrical and Electronics Research (IJEER)
Open Access | Rapid and quality publishing
Research Article | Volume 13, Issue 3 | Pages 487-492 | e-ISSN: 2347-470X

3.5. Plot of Gain in relation to Frequency

Figures 8 and *9* show the plots of gain in 2D and 3D modes. These plots may be viewed in the relevant figures. *Figure 8* makes it abundantly clear that the suggested antenna achieves a gain value of around 6 dB, or 5.92 dB to be precise, while operating at a centre frequency of 3 GHz. Taking into consideration that this figure is applicable for vast range of broadband wireless applications.

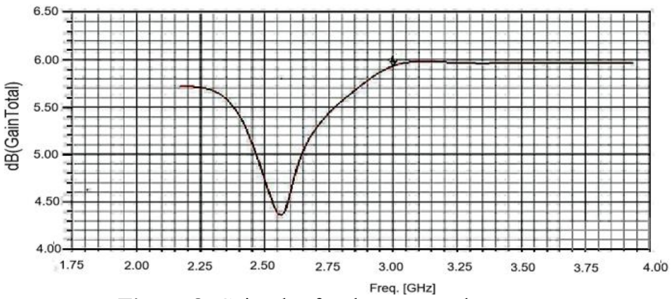

Figure 8. Gain plot for the proposed antenna

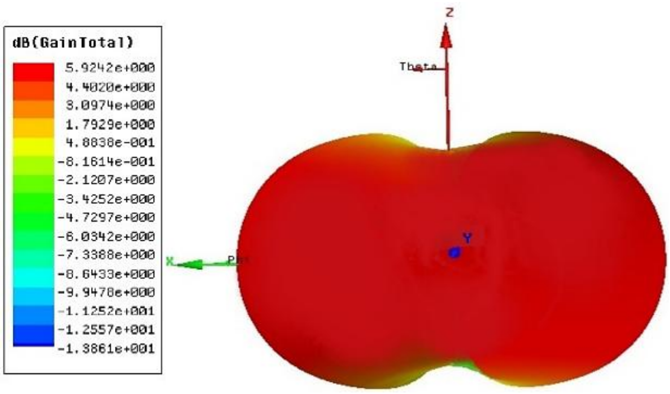

Figure 9. 3D gain distribution of proposed antenna

3.6. Efficiency of Proposed Design

Efficiency is a measure of the accurate way an antenna transforms electrical power into radiated electromagnetic waves. Efficiency is influenced by several variables, which includes the antenna design, the characteristics of the external environment, and any losses occurring inside the antenna structure. Having high antenna efficiency (η) is advantageous because it guarantees that a substantial amount of the input power is transformed into useable radiated energy, reducing power wastage and maximising the antenna efficiency for communication or detection purposes as seen in *table 2.*

Table 2. Parametric Analysis of proposed design

Reso. Freq. (GHz)	s_{11} (dB)	Gain (dB)	Imp. BW (%)	$\|R_i\|$ (dB)	VSWR	η (%)
3.0	-31.25	5.92	43.33	12	1.03	99.98

3.7. Comparison of the various Parameters of the designed Antenna

The dimensions of the proposed structure are compared to determine the extent of increase in bandwidth for each resonant frequency. *Figure 10* displays a bar graph comparing different antenna dimensions. It is important to note that in this figure, the bandwidth improvement for 3 GHz is zero, since this number is used as a reference. *Table 3* shows parametric analysis of this design with state-of-the-art studies.

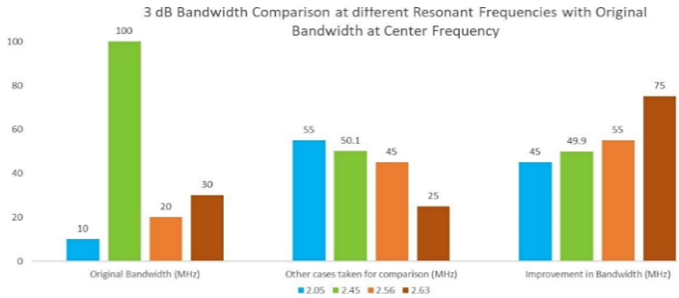

Figure 10. Bar graph comparison between varied antenna parameters

Table 3. Comparison of Parametric Analysis of this design and state-of-the-art literature

Ref.	Reso. Freq. (GHz)	VSWR	$\|R_i\|$ (dB)	Gain (dB)	BW (%)	Rad. Patt. Symm.
[8]	2.7	1.12	7	3.9	7.02	No
[23]	3.0	1.1	8.6	3.72	40	Yes
[22]	2.64	1.16	N.A.	2.87	20.83	N.A.
This design	3.0	1.03	12	5.92	43.33	Yes

4. HARDWARE ANTENNA MODEL FABRICATION & EXPERIMENTAL RESULTS USING VNA

The depicted configuration of the antenna is seen in *figure 11*, with precise dimensions matching those of the simulated model. The model was first created using Ansoft HFSS software, and subsequently, the design was printed on glossy paper. Subsequently, the design part was finalized and affixed onto a Rogers RT/duroid 5880 substrate with the allocated measurements. This was then followed by the procedure of chemical etching, which served to remove any surplus metal from the substrate, leaving just the desired design intact. There are *minor discrepancies* between the *simulated* and *measured* findings of the proposed antenna, as seen from graphs in *figures 12* and *13*. These differences may be attributed to the impact of *soldering* on the antenna, which is the primary cause of these variations. The whole process of simulating the suggested model and fabricating it to achieve the observed results is succinctly described using a design flowchart in *figure 14*.

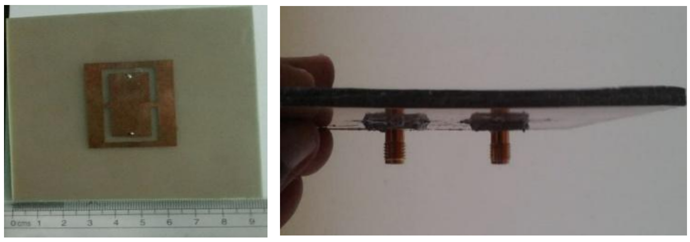

(a) (b)

Figure 11. Hardware model of the Patch Antenna with (a) Slotted Design view, (b) 3D view of attached connectors

Open Access | Rapid and quality publishing
International Journal of
Electrical and Electronics Research (IJEER)
Research Article | Volume 13, Issue 3 | Pages 487-492 | e-ISSN: 2347-470X

4.1. Explanation of results highlighting on novelty of design

By addressing the pertinent difficulty of limited bandwidth, which has traditionally hampered the operational efficacy of microstrip patch antennas (MPAs), the proposed work presents a noticeable and significant advancement in the design of MPAs. This study uses a dual-fed architecture with strategically placed inverted U-shaped slots, therefore transcending conventional techniques often based on single-feed methods or basic geometric changes. This dual mechanism highlights a major change from conventional design approaches by concurrently simulating many iterative modes, hence improving bandwidth enhancement. Apart from the arrangement of these elements, the *novelty* resides in the ingenious integration of slot and feed placement along with meticulous numerical refining of patch sizes. The result produces a resonant frequency that precisely corresponds with the center frequency of 3 GHz, thereby attaining a significant outcome guaranteeing good impedance matching and reduced signal reflection losses. Rarely is a performance profile obtained in patch antenna designs by the acquired broad impedance bandwidth, low VSWR, and gain.

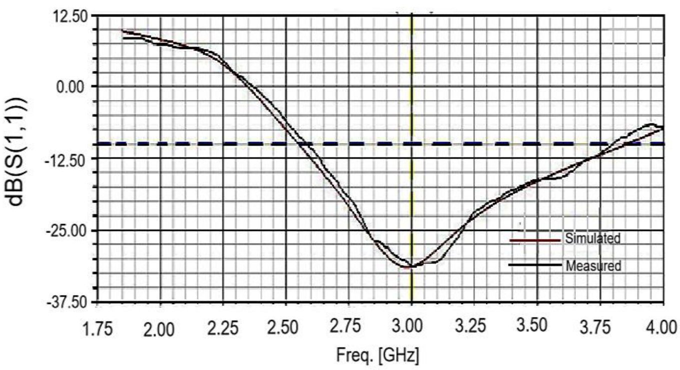

Figure 12. Comparison between Measurement and Simulation Results for return loss for Proposed Antenna

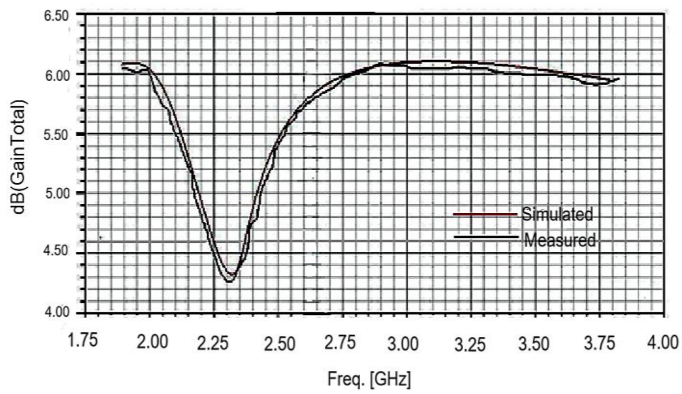

Figure 13. Comparison between Measurement and Simulation Results for Gain vs Frequency for Proposed Antenna

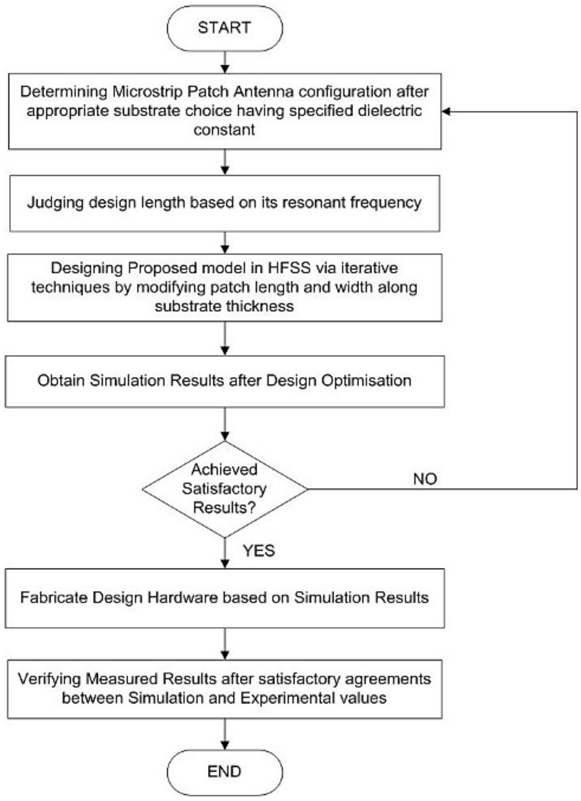

Figure 14. Flowchart for Proposed Model starting from simulation in HFSS upto obtainment of measured results

5. ANALYSIS OF THE RESULTS

The outcomes of this research confirm the effectiveness of the proposed dual-fed microstrip patch antenna (MPA) design in attaining wide bandwidth and high efficiency, which are essential factors for modern wireless communication systems. The integration of two symmetrically positioned inverted U-shaped slots along with dual coaxial probe feeds has resulted in a significant improvement in the antenna's impedance bandwidth, ≈ 44% within the 2.55 GHz to 3.85 GHz frequency range. This is essential as it guarantees peak performance while minimizing signal degradation at the desired frequency. The remarkably low Voltage Standing Wave Ratio (VSWR ≈ 1) underscores the effective impedance matching of the proposed design, reducing signal reflection and enhancing power transmission. The analysis of comparative performance across various configurations highlights the significance of strategic slot positioning and dimension tuning in enhancing bandwidth extension and achieving precision in resonant frequency. The coherence between simulated outcomes from HFSS, utilizing the Finite Element Method (FEM), and actual measurements acquired through a vector network analyzer (VNA) post-fabrication *via* chemical etching, confirms the strength and dependability of the design process. The robust correlation underscores the appropriateness of the simulation methodology for subsequent design optimization efforts.

6. CONCLUSION

This study efficiently addresses the fundamental limitation of narrow bandwidth found in traditional microstrip patch antennas through the introduction of an innovative design methodology. The integration of a pair of inverted U-shaped slots and a dual coaxial probe feed, combined with a systematic numerical optimization of patch dimensions, results in a notable enhancement of bandwidth for the antenna. The resonant frequency is precisely aligned with the center frequency of 3GHz, which guarantees excellent impedance matching and efficient operation. The final design achieves an impressive impedance bandwidth of 43.33%, a low VSWR of 1.03, and a robust radiation intensity of 12dB. The antenna also demonstrates a symmetrical radiation pattern and a gain nearing 6 dB, which renders it particularly appropriate for use in the S-band (2–4 GHz) spectrum. The outcomes were confirmed through comprehensive iterative simulations utilizing Ansoft HFSS, supporting the proposed antenna's suitability for present day wireless systems such as WLAN, WiMAX, 5G, and IoT applications.

REFERENCES

[1] Tanvir Islam, Esraa Mousa Ali, Wahaj Abbas Awan, Mohammed S. Alzaidi, Thamer AH Alghamdi, and Moath Alathbah. "A parasitic patch loaded staircase shaped UWB MIMO antenna having notch band for WBAN applications." Heliyon 10(1) (2024).

[2] Youngje Sung. "Simple patch antenna with filtering function using two U-slots." Journal of Electromagnetic Engineering and Science 21(5), 425-429 (2021).

[3] O. W. Ata, M. Salamin, and K. Abusabha, Double U-Slot Rectangular Patch Antenna for Multiband Applications, Elsevier 84, 106608 (2020).

[4] T. Q. Fan, B. Jiang, R. Liu, J. Xiu, Y. Lin, and H. Xu, A Novel Double U-Slot Microstrip Patch Antenna Design for Low-Profile and Broad Bandwidth Applications, IEEE Transac. on Antennas & Propag. 70(4), 2543-2549 (2021).

[5] Md Mottahir Alam, Md Siam Talukder, Md Samsuzzaman, Asif Irshad Khan, Navin Kasim, Ibrahim Mustafa Mehedi, and Rezaul Azim. "W-shaped slot-loaded U-shaped low SAR patch antenna for microwave-based malignant tissue detection system." Chinese Journal of Physics 77, 233-249 (2022).

[6] V. A. P. Chavali and A. A. Deshmukh, Half U-Slot and Rectangular Slot Loaded Nearly Square Microstrip Antennas for Wideband Response, Progress in Electromagnetics Research C 104, 129-141 (2020).

[7] M. T. Nguyen, Y. F. Lin, C. H. Chang, C. H. Chen, and H. M. Chen, Compact Shorted C-Shaped Patch Antenna for Ultrahigh Frequency Radio Frequency Identification Tags Mounted on a Metallic Plate, International Journal of RF and Microwave Computer-Aided Engineering 31(6), e22595 (2021).

[8] L. Song, W. Gao, and Y. Rahmat-Samii, 3-D Printed Microfluidics Channelizing Liquid Metal for Multipolarization Reconfigurable Extended E-Shaped Patch Antenna, IEEE Transactions on Antennas and Propagation 68(10), 6867-6878 (2020).

[9] J. F. Lin and L. Zhu, Bandwidth and Gain Enhancement of Patch Antenna Based on Coupling Analysis of Characteristic Modes, IEEE Transactions on Antennas and Propagation 68(11), 7275-7286 (2020).

[10] A. S. Das, A. Goel, and S. Nakhate, Performance analysis of wideband microstrip patch antenna with amplified radiation, Microsystem Technologies, 28(11), 2429-2441 (2022).

[11] B. Mishra, R. K. Verma, N. Yashwanth, and R. K. Singh, A review on microstrip patch antenna parameters of different geometry and bandwidth enhancement techniques, International Journal of Microwave and Wireless Technologies, 14(5), 652-673 (2022).

[12] M. A. Haque, M. A. Zakariya, N. S. S. Singh, M. A. Rahman, and L. C. Paul. Parametric study of a dual-band quasi-Yagi antenna for LTE application. Bulletin of Electrical Engineering and Informatics, 12(3), 1513-1522 (2023).

[13] M. M. Shirkolaei, Wideband Linear Microstrip Array Antenna with High Efficiency and Low Side Lobe Level, International Journal of RF and Microwave Computer-Aided Engineering 30(11), e22412 (2020)

[14]. A. S. Das, A. Goel, and S. Nakhate, A wideband stacked microstrip patch antenna design with augmented gain-bandwidth product for 5G wireless applications, Sādhanā, 48(4), 284 (2023).

[15] A. S. Das, A. Goel, S. Nakhate, D. Mitra, and Y. K. Gupta, Wideband Patch Antenna for Stable Radiation Pattern Generation. Paper presented at the 2023 1st International Conference on Innovations in High-Speed Communication and Signal Processing (IHCSP), Bhopal, India, March 2023, pp. 407-410. IEEE

[16] Q. Q. Li, H. Pan, Z. H. Zhao, and H. F. Zhang, A Circularly Polarized Antenna Array with Sequential-Phase Feed Network, Journal of Electromagnetic Waves and Applications 36(9), 1244- 1256 (2022).

[17] C. A. Balanis, Antenna Theory: Analysis and Design (John wiley & sons, 2016).

[18] C. Güler, S. E. B. Keskin, and R. B. Aymaz, The development of broadband microstrip patch antenna for wireless applications, Bitlis Eren University Journal of Science 11(3), 812-819 (2022).

[19] A. Ghaffar, X. J. Li, W. A. Abbas Awan, S. I. Iffat Naqvi, N. Hussain, B. C. Seet, and E. Limiti, Design and Realization of a Frequency Reconfigurable Multimode Antenna for ISM, 5G-Sub-6-GHz, and S-Band Applications, Applied Sciences 11(4), 1635 (2021).

[20] M. Wang, Q. Zhu, and C. H. Chan, Wideband, Low-Profile Slot-Fed Dipole-Patch Antenna and Array, IEEE Antennas and Wireless Propagation Letters 19(12), 2250-2254 (2020).

[21] P. Bouca, J. N. Matos, S. R. Cunha, and N. B. Carvalho, Low-Profile Aperture-Coupled Patch Antenna Array for CubeSat Applications, IEEE Access 8, 20473-20479 (2020).

[22] S. C. Tang, X. Y. Wang, W. W. Yang, and J. X. Chen, Wideband Low-Profile Dielectric Patch Antenna and Array with Anisotropic Property, IEEE Transac. on Antennas & Propag. 68, 4091 (2019).

[23] M. Li, Y. Yang, F. Iacopi, J. Nulman, and S. Chappel-Ram, 3D-Printed Low-Profile Single-Substrate Multi-Metal Layer Antennas and Array with Bandwidth Enhancement, IEEE Access 8, 217370- 217379 (2020).